Eur. Phys. J. C 53, 585–589 (2008)
DOI 10.1140/epjc/s10052-007-0500-7

THE EUROPEAN PHYSICAL JOURNAL C

Regular Article – Theoretical Physics

# Universal behavior of transverse momentum distributions of baryons and mesons in the framework of percolation of strings

L. Cunqueiro[1,2,a], J. Dias de Deus[3], E.G. Ferreiro[1,2], C. Pajares[1,2]

[1] Instituto Galego de Física de Altas Enerxías, Facultad de Física, Universidade de Santiago de Compostela, Campus Sur s/n, 15782 Santiago de Compostela, Spain
[2] Departamento de Física de Partículas, Universidade de Santiago de Compostela, 15782 Santiago de Compostela, Spain
[3] CENTRA, Instituto Superior Técnico, 1049-001 Lisboa, Portugal

Received: 2 August 2007 / Revised version: 20 August 2007 /
Published online: 8 January 2008 – 

**Abstract.** In the framework of percolation of strings, the transverse momentum distributions in $AA$ and $hh$ collisions at all centralities and energies show a universal behavior. The width of these distributions is related to the width of the distribution of the size of the clusters formed by the overlapping of the strings produced. The difference between the distributions for baryons and mesons originates in the fragmentation of clusters of several strings, which enhances the particles with a higher number of constituents. The results agree with SPS and RHIC data. The predictions for LHC show differences for baryons compared with RHIC. At LHC energies we obtain also a high $p_{\mathrm{T}}$ suppression for $pp$ high multiplicity events compared with the $pp$ minimum bias.

**PACS.** 25.75.Nq; 12.38.Mh; 24.85.+p

Multiparticle production can be described in terms of color strings stretched between the partons of the projectile and target. These strings decay into new ones by sea $q$–$\bar{q}$ pair production and subsequently hadronize to produce the observed hadrons. The color in these strings is confined to a small area in transverse space: $S_1 = \pi r_0^2$ with $r_0 \simeq 0.2$–$0.3$ fm. With increasing energy and/or atomic number of the colliding particles, the number of exchanged strings grows, and they start to overlap, forming clusters, very much like disks in two-dimensional percolation theory. At a certain critical density, a macroscopical cluster appears, which marks the percolation phase transition [1–4]. For nuclear collisions, this density corresponds to the value of $\eta = N_{\mathrm{S}}\frac{S_1}{S_A}$ of $\eta_{\mathrm{C}} = 1.18$–$1.5$ (depending of the type of profile functions employed), where $N_{\mathrm{S}}$ is the number of strings and $S_A$ corresponds to the overlapping area of the nuclei. A cluster of $n$ strings behaves as a single string with an energy-momentum that corresponds to the sum of the energy-momentum of the overlapping strings and with a higher color field, corresponding to the vectorial sum of the color fields of the individual strings. In this way, the multiplicity $\langle\mu_n\rangle$ and the mean transverse momentum squared $\langle p_{\mathrm{T}}^2\rangle_n$ of the particles produced by a cluster are given by

$$\langle\mu\rangle_n = \sqrt{\frac{nS_n}{S_1}}\langle\mu\rangle_1\,, \quad \langle p_{\mathrm{T}}^2\rangle_n = \sqrt{\frac{nS_1}{S_n}}\langle p_{\mathrm{T}}^2\rangle_1\,, \qquad (1)$$

where $\langle\mu\rangle_1$ and $\langle p_{\mathrm{T}}^2\rangle_1$ stand for the mean multiplicity and mean $p_{\mathrm{T}}^2$ of particles produced in a single string. Equations (1) transform into analytical ones [3, 4] in the limit of random distributions of strings:

$$\langle\mu\rangle = N_{\mathrm{S}}F(\eta)\langle\mu\rangle_1\,, \quad \langle p_{\mathrm{T}}^2\rangle = \frac{\langle p_{\mathrm{T}}^2\rangle_1}{F(\eta)}\,, \qquad (2)$$

where $F(\eta) = \sqrt{\frac{1-\mathrm{e}^{-\eta}}{\eta}}$. If we are interested in a certain kind of particle $i$, we will use $\langle\mu\rangle_{1i}$, $\langle p_{\mathrm{T}}^2\rangle_{1i}$, $\langle\mu\rangle_{ni}$ and $\langle p_{\mathrm{T}}^2\rangle_{ni}$ for the corresponding quantities. The transverse momentum distributions can be written as a superposition of the transverse momentum distributions of each cluster, $g(x, p_{\mathrm{T}})$, weighted with the distribution of the different tensions of the clusters, i.e. the distribution of the size of the clusters, $W(x)$ [5–7]. For $g(x, p_{\mathrm{T}})$ we assume the Schwinger formula $g(x, p_{\mathrm{T}}) = \exp\left(-p_{\mathrm{T}}^2 x\right)$ and for the weight function $W(x)$ the gamma distribution $W(x) = \frac{\gamma}{\Gamma(k)}(\gamma x)^{k-1}\exp(-\gamma x)$, where

$$\gamma = \frac{k}{\langle x\rangle}\,, \quad \frac{1}{k} = \frac{\langle x^2\rangle - \langle x\rangle^2}{\langle x\rangle^2}\,.$$

$x$ is proportional to the inverse of the tension of each cluster, or stated precisely, $x = 1/\langle p_{\mathrm{T}}^2\rangle_n = \sqrt{\frac{S_n}{nS_1}}\frac{1}{\langle p_{\mathrm{T}}^2\rangle}$. $k$ is proportional to the inverse of the width of the distribution on $x$ and depends on $\eta$, the density of strings. Therefore, the

[a] e-mail: leticia@fpaxp1.usc.es

transverse momentum distribution $f(p_{\mathrm{T}}, y)$ is

$$\frac{\mathrm{d}N}{\mathrm{d}p_{\mathrm{T}}^2\,\mathrm{d}y} = f(p_{\mathrm{T}}, y) = \int_0^\infty \mathrm{d}x W(x) g(p_{\mathrm{T}}, x) = \frac{\mathrm{d}N}{\mathrm{d}y}\frac{k-1}{k}\frac{1}{\langle p_{\mathrm{T}}^2\rangle_{1i}} F(\eta) \frac{1}{\left(1+\frac{F(\eta)p_{\mathrm{T}}^2}{k\langle p_{\mathrm{T}}^2\rangle_{1i}}\right)^k}. \quad (3)$$

Equation (3) is valid for all densities and types of collisions. It only depends on the parameters $\langle p_{\mathrm{T}}\rangle_{1i}$ and $k$. At low density, there is no overlap between strings and there are no fluctuations on the string tension; all the clusters have one string. Therefore, $k$ goes to infinity, and $f(p_{\mathrm{T}}, y) \simeq \exp\left(-\frac{p_{\mathrm{T}}^2}{\langle p_{\mathrm{T}}^2\rangle_1}\right)$. At very high density $\eta$, there is only one cluster formed by all the strings produced. Again, there are no fluctuations, $k$ tends to infinity and $f(p_{\mathrm{T}}, y) \simeq \exp\left(-\frac{F(\eta)p_{\mathrm{T}}^2}{\langle p_{\mathrm{T}}^2\rangle_1}\right)$. In between these two limits, $k$ has a minimum for intermediate densities corresponding to the maximum of the cluster size fluctuations. This behavior of $k$ with $\eta$ [5–7] is related to the behavior with centrality of the transverse momentum [8–10] and multiplicity fluctuations [11, 12]. We observe from (3) that

$$\frac{\mathrm{d}\ln f(p_{\mathrm{T}}^2, y)}{\mathrm{d}\ln p_{\mathrm{T}}} = -\frac{2F(\eta)}{\left(1+\frac{2F(\eta)p_{\mathrm{T}}^2}{k\langle p_{\mathrm{T}}^2\rangle_i}\right)}\frac{p_{\mathrm{T}}^2}{\langle p_{\mathrm{T}}^2\rangle_{1i}}. \quad (4)$$

As $p_{\mathrm{T}}^2 \to 0$, (4) reduces to $\frac{-2F(\eta)p_{\mathrm{T}}^2}{\langle p_{\mathrm{T}}^2\rangle_i}$, while for larger $p_{\mathrm{T}}$ it becomes $-2k$ for all particle species. As $\langle p_{\mathrm{T}}^2\rangle_{1p} \geq \langle p_{\mathrm{T}}^2\rangle_{1K} \geq \langle p_{\mathrm{T}}^2\rangle_{1\pi}$, the absolute value is larger for pions than for kaons and for protons, in agreement with the experimental data [5].

The nuclear modification factor, defined by $R_{AA}(p_{\mathrm{T}}) = \frac{\mathrm{d}N^{AA}}{\mathrm{d}p_{\mathrm{T}}^2\,\mathrm{d}y} / N_{\mathrm{coll}}\frac{\mathrm{d}N^{pp}}{\mathrm{d}p_{\mathrm{T}}^2\,\mathrm{d}y}$, reduces to the following expression at $p_{\mathrm{T}}^2 = 0$ (we use (2) for $\frac{\mathrm{d}N}{\mathrm{d}y}$):

$$R_{AA}(0) \sim \left(\frac{F(\eta')}{F(\eta)}\right)^2 < 1, \quad (5)$$

where $\eta'$ and $\eta$ are the corresponding densities for nucleus–nucleus collisions and $pp$ collisions, respectively. $\eta' > \eta$; thus $F(\eta') < F(\eta)$. As $p_{\mathrm{T}}$ increases we have

$$R_{AA}(p_{\mathrm{T}}) \sim \frac{1+F(\eta)\frac{p_{\mathrm{T}}^2}{\langle p_{\mathrm{T}}^2\rangle_{1i}}}{1+F(\eta')\frac{p_{\mathrm{T}}^2}{\langle p_{\mathrm{T}}^2\rangle_{1i}}}\left(\frac{F(\eta')}{F(\eta)}\right)^2, \quad (6)$$

and $R_{AA}$ increases with $p_{\mathrm{T}}$ up to a maximum value. At larger $p_{\mathrm{T}}$ ($\frac{p_{\mathrm{T}}^2}{k\langle p_{\mathrm{T}}^2\rangle_{1i}}F(\eta) > 1$)

$$R_{AA} \sim p_{\mathrm{T}}^{2(k(\eta)-k'(\eta'))}. \quad (7)$$

At high density $k'(\eta') > k(\eta)$ and suppression of $p_{\mathrm{T}}$ occurs.

The universal formula (3) must be regarded as an analytical approximation to a process that consists of the formation of clusters of strings and their eventual decay via the Schwinger mechanism. We do not claim to have an alternative description valid at all $p_{\mathrm{T}}$. It is well known that jet quenching is the working mechanism responsible for the high $p_{\mathrm{T}}$ suppression. This phenomenon is not included in our formula, which was obtained assuming a single exponential for the decay of a cluster without a power-like tail. Our work must be considered as a way of interpolating and of joining smoothly the low and intermediate $p_{\mathrm{T}}$ region with the high $p_{\mathrm{T}}$ region. The suppression of high $p_{\mathrm{T}}$ is in correspondence with a modification in the behavior at intermediate $p_{\mathrm{T}}$, and this is what we study. Although it describes many of the observed features of the experimental SPS and RHIC data, it is not able to explain the differences between antibaryons (baryons) and mesons. In fact, the only parameter that is different for them in (3) is the mean transverse momentum of pions and protons produced by a single string $\langle p_{\mathrm{T}}^2\rangle_{1\pi}$ and $\langle p_{\mathrm{T}}^2\rangle_{1p}$, respectively. This only causes a shift of the maximum of $R_{AA}$ but keeps the same height at the maximum contrary to what one observed. However, in the fragmentation of a cluster formed by several strings, the enhancement of the production of antibaryons (baryons) over mesons is not only due to a mass effect corresponding to a higher tension due to a higher density of the cluster (the factor $F(\eta)$ in front of $p_{\mathrm{T}}^2$ in (3)). In fact, the color and flavor properties of a cluster follow from the corresponding properties of their individual strings. A cluster composed of several quark–antiquarks ($q$–$\bar{q}$) strings behaves like a ($q$–$\bar{q}$) string, with a color $Q$ and flavor composed of the flavor of the individual strings. As a result, we obtain clusters with higher color and differently flavored ends. For the fragmentation of a cluster we consider the creation of a pair of parton complexes $Q\bar{Q}$ [13]. After the decay, the two new $Q\bar{Q}$ strings are treated in the same manner and therefore decay into more $Q\bar{Q}$ strings, until they come to objects with masses comparable to hadron masses, which are identified with observable hadrons by combining with them the produced flavor with statistical weights. In this way, the production of antibaryons (baryons) is enhanced with the number of strings of the cluster. As an example, in Fig. 1 we show the results for the decay of a color octet cluster and color sextet formed by two 3–$\bar{3}$ strings [13], where there is a large enhancement of antibaryons (baryons). Notice that the enhancement of strangeness with zero baryon number is smaller [13–16]. We observe that the additional antiquarks (quarks) required to form an (anti-) baryon are provided by the antiquarks (quarks) of the overlapping strings that form the cluster. In this way, the ideas of recombination and coalescence [17–21] are naturally incorporated in our approach. In order to take this into account in our formulas, we must modify (1)–(3). For (anti-) baryons we will consider the multiplicity per unit of rapidity to be instead of the first equation of (2):

$$\mu_{\overline{B}} = N_{\mathrm{S}}^{1+\alpha} F(\eta_{\overline{B}}) \mu_{1\overline{B}} \quad (8)$$

fitting the parameter $\alpha$ to reproduce the experimental dependence of the $p_{\mathrm{T}}$ integrated $\bar{p}$ spectra with centrality [22]. The result is shown in Fig. 2 and the obtained values are $\alpha = 0.09$ and $\frac{\mu_{1\bar{p}}}{\mu_{1\bar{\pi}}} = \frac{1}{30}$. Here $\mu_{1\bar{p}}$ and $\mu_{1\bar{\pi}}$ are the

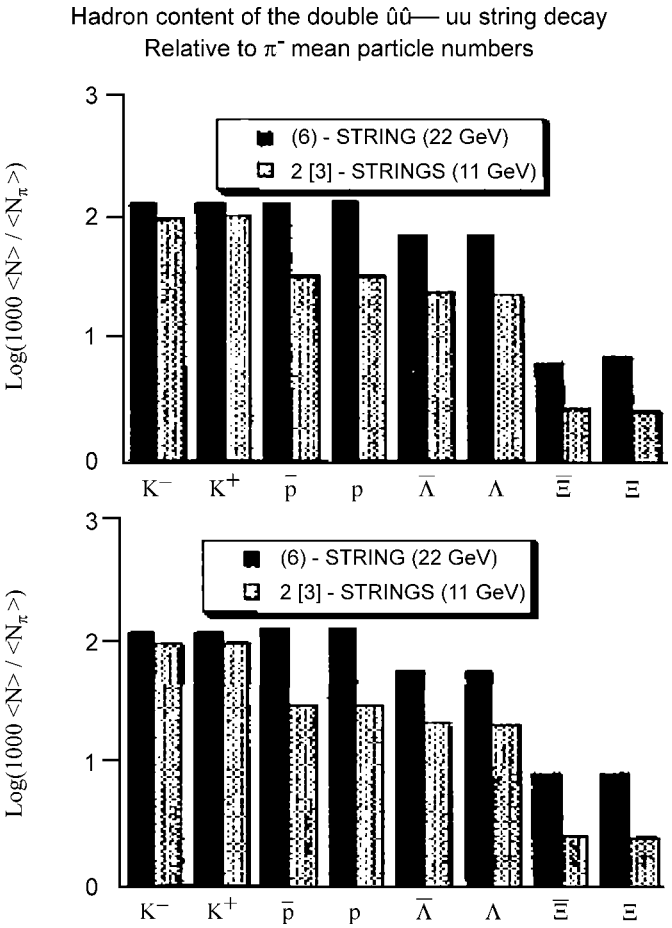


**Fig. 1.** Hadronic content of the decay of octet and sextet strings relative to the number of $\pi^-$

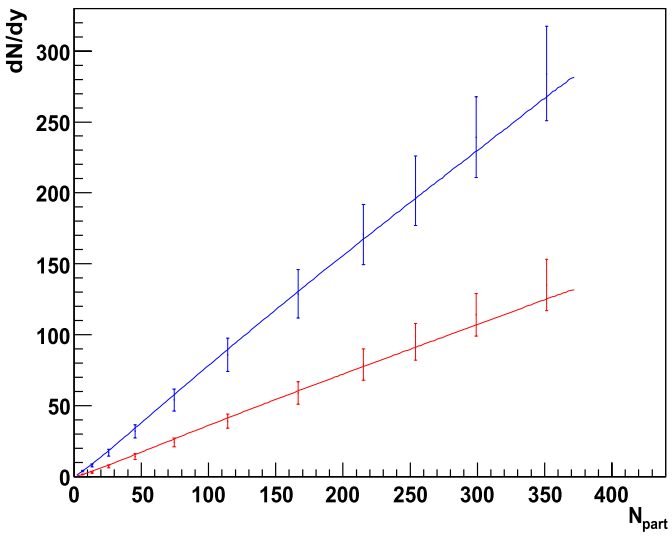


**Fig. 2.** $p_{\mathrm{T}}$ integrated antiproton (*red*, $\times 10$) and neutral pion (*blue*) spectra as a function of centrality compared to the PHENIX data

mean multiplicity of a single string for antiprotons and pions, respectively. It is observed that when an antibaryon is triggered, the effective number of strings is $N_{\mathrm{S}}^{1+\alpha}$ instead of $N_{\mathrm{S}}$. This means that the density $\eta$ must be replaced by $\eta_{\overline{B}} = N_{\mathrm{S}}^{\alpha}\eta$. The (anti-) baryons probe a higher density than mesons for the same energy and type of collision. On the other hand, from the constituent counting rules [23–25] it is expected that the power-like $p_{\mathrm{T}}$ behavior for baryons is suppressed in one half more than for mesons. Therefore, in (3) we must use for (anti-) baryons $\eta_B$ and the corresponding functions $F(\eta_B)$ and $k_B = k(\eta_B) + \frac{1}{2}$. Since $\eta_B > \eta$ we have $F(\eta_B) < F(\eta)$ and $k(\eta_B) > k(\eta)$. For peripheral collisions, $N_{\mathrm{S}}^{\alpha}$ is smaller than for central collisions and $\eta_B$ is more similar to $\eta$. Therefore, the differences between the transverse momentum distributions are smaller, as is shown by the experimental data. In order to compute the different $\eta$ for different centralities, we use the Monte Carlo code of [13, 14]. Their values at RHIC and LHC and their corresponding $k$ are tabulated below. Note that the values of $k$ come from the universal function that gives the shape of the dependence of $k$ on $\eta$ [5–7].

In our approach, we should use a different $\alpha$ for baryons and antibaryons as far as the increase with centrality is slightly different for both, depending also on the specific kind of baryon (antibaryon). In order to obtain a single formula we considered strings of the same type. However, usually two types of strings are considered. One has strings $qq$–$q$ or $q$–$qq$, which stretch a diquark of the projectile (target) with a quark of the target (projectile) and strings $q$–$\bar{q}$ or $\bar{q}$–$q$, linking quarks and antiquarks. The fragmentation of the strings of the type $qq$–$q$ or $q$–$qq$ favors the production of baryons over antibaryons in the fragmentation regions of the projectile and the target. Therefore, our results should be limited to the central rapidity region. On the other hand, we have determined $\alpha$ from the dependence of $\frac{\bar{p}}{\pi}$ with centrality. The large error data translate into uncertainties in $\alpha$ of the order of 20%, which is of the same order as the differences in the parameter $\alpha$ for baryons and antibaryons. The uncertainties in $\alpha$ induce uncertainties in the determination of $\eta_B$ and hence in $k_B$; these uncertainties are however negligible (less than 5% even at the highest centrality). We conclude that our single formula using the same $\alpha$ for baryons and antibaryons is a good approximation.

On the other hand, we have assumed an additional difference between baryons and mesons, $k_B = k(\eta_B) + 1/2$,

**Table 1.** Density of strings and the corresponding $k$ values for mesons and baryons at RHIC and LHC

| Centrality | $\eta$ | $k$ | $\eta_B$ | $k_B$ |
|---|---|---|---|---|
| | | RHIC | | |
| Au–Au 0%–10% | 2.69 | 3.97 | 5.17 | 4.82 |
| Au–Au 60%–92% | 0.9 | 3.58 | 1.24 | 4.16 |
| Au–Au 80%–92% | 0.6 | 3.55 | 0.75 | 4.06 |
| *pp* | 0.4 | 3.60 | 0.48 | 4.07 |
| | | LHC | | |
| Au–Au 0%–10% | 4.85 | 4.07 | 9.8 | 4.99 |
| Au–Au 60%–92% | 1.62 | 3.56 | 2.34 | 4.21 |
| Au–Au 80%–92% | 1.08 | 3.44 | 1.43 | 4.02 |
| *pp* | 0.72 | 3.38 | 0.92 | 3.90 |

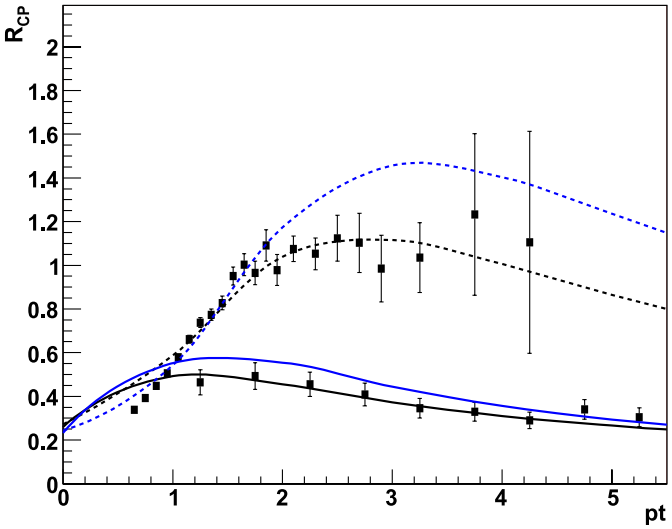


**Fig. 3.** $R_{CP}$ (0%–10% central/60%–92% peripheral) for pions (*solid line*) and $(p+\bar{p})/2$ (*dashed*) compared to the PHENIX data. In *blue*, LHC predictions

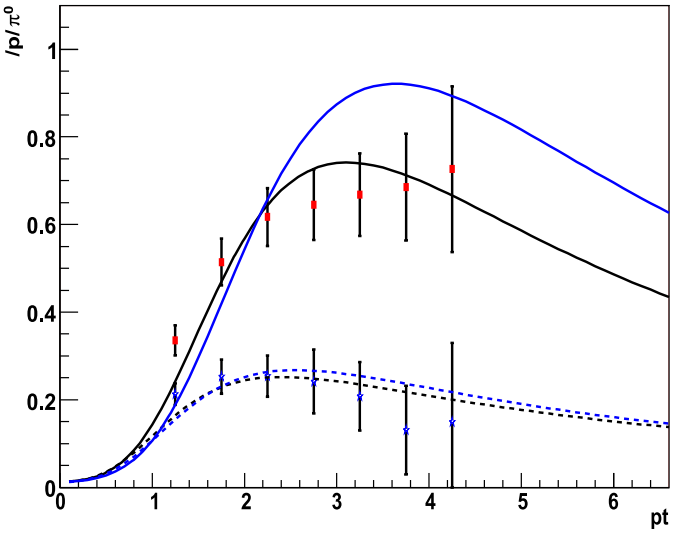


**Fig. 4.** Antiproton to neutral pion ratio as a function of $p_{\mathrm{T}}$ for 0%–10% (*solid*) and 60%–92% (*dashed*) centrality bins compared to the PHENIX data. LHC predictions in *blue*

from the high $p_{\mathrm{T}}$ behavior of (3). This could seem inconsistent with our approach, which is limited to low and intermediate $p_{\mathrm{T}}$. As we have said above, our goal is not to give a full description of the data, including high $p_{\mathrm{T}}$, but an alternative description of intermediate $p_{\mathrm{T}}$ suppression. In this way, this factor can be seen as a boundary condition imposed on our approach. Notice that this factor is independent of the centrality, and therefore its influence on the ratios $R_{CP}$ and $R_{AA}$ is not large. In fact, if we use for $k_B$ the values without the factor 1/2, $R_{CP}$ is smaller at $p_{\mathrm{T}} = 2\,\mathrm{GeV}/c$ and $p_{\mathrm{T}} = 10\,\mathrm{GeV}/c$ in a factor 1.13 and 1.25 respectively at RHIC energies. This small reduction does not spoil the agreement with the data, although a better agreement at high $p_{\mathrm{T}}$ is obtained with the factor 1/2.

In Fig. 3, we show our results for the ratio $R_{CP}$ in Au–Au collisions defined as usual, for $(p+\bar{p})/2$ (dashed line) and neutral pions (solid line), compared to the PHENIX [22] experimental data. We find a good agreement. We also show the LHC prediction for pions and antiprotons. There is no change for pions but on the contrary, the difference between antibaryons and pions is enhanced. In Fig. 4 we show the $p_{\mathrm{T}}$ dependence of the ratio $\frac{\bar{p}}{\pi^0}$ for peripheral (dashed line) and central (solid line) Au–Au collisions together with the experimental data [22]. LHC predictions are also shown. The difference only appears for central collisions.

In Fig. 5 we show our results for the modified nuclear factor $R_{AA}$ for pions (solid lines) and protons (dashed lines) for peripheral and central collisions together with the experimental data for pions [26]. Again, the main difference arises for central collisions. In Fig. 6, this difference between pions and protons is compared at RHIC and LHC energies. The Cronin effect becomes larger at LHC for protons, contrary to some expectations [27].

The good agreement obtained with the experimental data can be understood as two combined effects: the larger

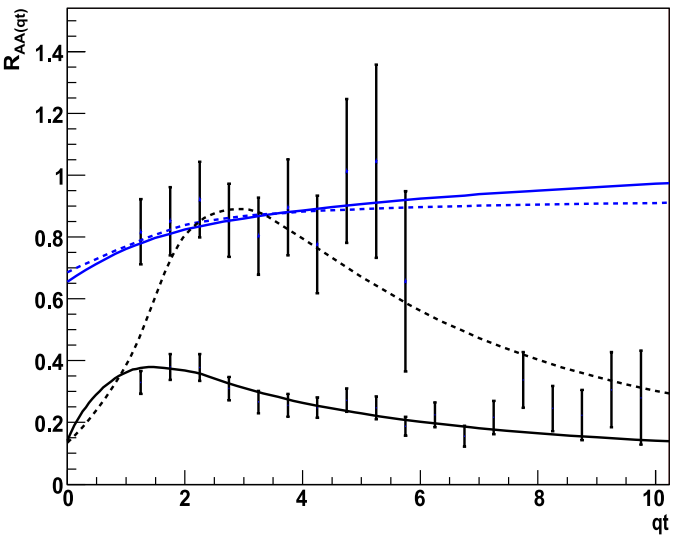


**Fig. 5.** Nuclear modification factor for neutral pions (*solid*) and protons (*dashed*) for 0%–10% central and 80%–92% peripheral bins compared to the PHENIX data

string tension of the cluster and the formation of strong color fields [28, 29] and the way of fragmentation of the clusters, which enhances the (anti-) baryon over mesons similarly to recombination models [17–21]. Both effects are widely recognized as working physical mechanisms at high densities. Both effects are naturally incorporated in the percolation of strings approach.

The shape of $R_{AA}$ and $R_{CP}$ has nothing to do with the nucleon structure of the nucleus an it depends essentially on the string density. One can wonder whether in $pp$ at LHC energies can be reached enough string densities to get a high $p_{\mathrm{T}}$ suppression. In Fig. 7 we answer this question. The ratio $R_{CP}$ is plotted between the inclusive $pp$ going to $\pi$, $k$ and $\bar{p}$ cross section for events with a multiplicity

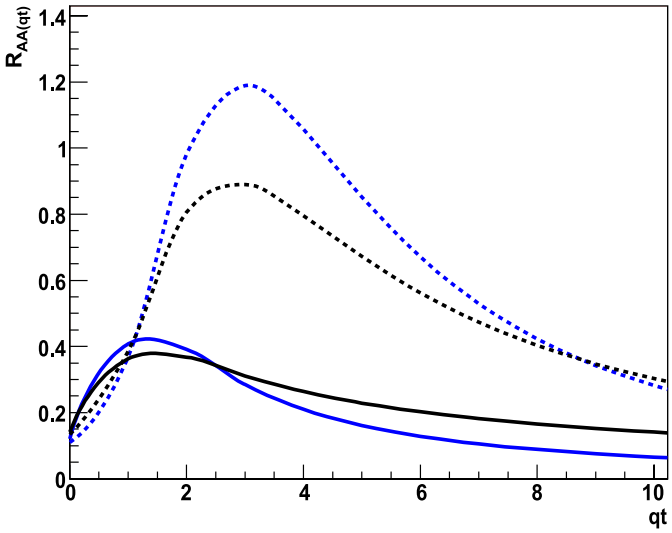


**Fig. 6.** Nuclear modification factor for 0%–10% central pions (*solid*) and protons (*dashed*) at RHIC (*black*) and LHC (*blue*)

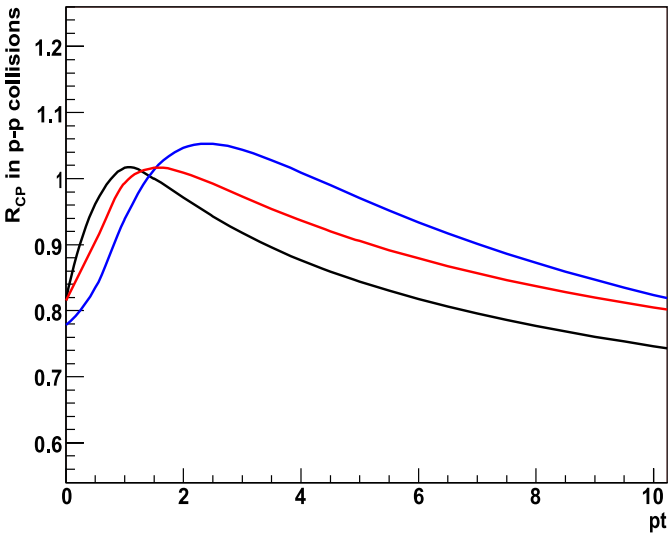


**Fig. 7.** Central to peripheral ratio for $pp$ collisions at LHC. *Black*: $\pi^0$, *red*: kaons, *blue*: $\bar{p}$

twice higher than the mean multiplicity and the minimum bias cross section. There is observed a suppression for $p_T$ larger than 3 GeV/$c$. However, the string density in $pp$ collisions reached will not be enough to suppress the back to back jet correlations as observed at RHIC energies for Au–Au central collisions. A straightforward evaluation following [5] gives a maximum of absorption of $\Delta p_T = 2$ GeV/$c$ for a number of strings of the order of 25–30, corresponding to events with a multiplicity twice the minimum bias multiplicity.

*Acknowledgements.* We thank the Ministerio de Educación y Ciencia of Spain under project FPA2005-01963 and Conselleria de Educación da Xunta de Galicia for financial support. We thank N. Armesto, C. Salgado and Y. Shabelski for discussions.

## References

1. N. Armesto, M.A. Braun, E.G. Ferreiro, C. Pajares, Phys. Rev. Lett. **77**, 3736 (1996)
2. M. Nardi, H. Satz, Phys. Lett. B **442**, 14 (1998)
3. M.A. Braun, C. Pajares, Phys. Rev. Lett. **85**, 4864 (2000)
4. M.A. Braun, C. Pajares, Eur. Phys. J. C **85**, 349 (2000)
5. J. Dias de Deus, E.G. Ferreiro, C. Pajares, R. Ugoccioni, Eur. Phys. J. C **40**, 229 (2005)
6. C. Pajares, Eur. Phys. J. C **43**, 9 (2005)
7. J. Dias de Deus, R. Ugoccioni, Eur. Phys. J. C **43**, 249 (2005)
8. PHENIX Collaboration, K. Adcox et al., Nucl. Phys. A **757**, 184 (2005)
9. E.G. Ferreiro, F. del Moral, C. Pajares, Phys. Rev. C **69**, 034 901 (2004)
10. J. Dias de Deus, A. Rodrigues, hep-ph/0308011
11. NA49 Collaboration, C. Alt et al., Phys. Rev. C **75**, 064 904 (2007)
12. L. Cunqueiro, E.G. Ferreiro, F. del Moral, C. Pajares, Phys. Rev. C **72**, 024 907 (2005)
13. N.S. Amelin, M.A. Braun, C. Pajares, Z. Phys. C **63**, 507 (1994)
14. N. Armesto, C. Pajares, D. Sousa, Phys. Lett. B **527**, 92 (2002)
15. H.J. Mohring, J. Ranft, C. Merino, C. Pajares, Phys. Rev. D **47**, 4142 (1993)
16. C. Greiner, AIP Conf. Proc. **644**, 337 (2003) [nucl-th/0208080]
17. R.C. Hwa, C.B. Yang, Phys. Rev. C **69**, 034 902 (2004)
18. V. Greco, C.M. Ko, P. Levai, Phys. Rev. Lett. **90**, 202 302 (2003)
19. R.J. Fries, B. Muller, C. Nonaka, S.A. Bass, Phys. Rev. Lett. **90**, 202 303 (2003)
20. R.J. Fries, B. Muller, C. Nonaka, S.A. Bass, Phys. Rev. C **68**, 044 902 (2003)
21. L. Maiani, A.D. Polosa, V. Riquer, C.A. Salgado, Phys. Lett. B **645**, 138 (2007)
22. PHENIX Collaboration, S.S. Adler et al., Phys. Rev. C **69**, 034 909 (2004)
23. S.J. Brodsky, G.R. Farrar, Phys. Rev. Lett. **31**, 1153 (1973)
24. V.A. Matreev, R.M. Murddyan, A.N. Tavkheldize, Lett. Nuovo Cimento **7**, 719 (1973)
25. G.P. Lepage, S.J. Brodsky, Phys. Rev. D **22**, 2157 (1980)
26. PHENIX Collaboration, S.S. Adler et al., Phys. Rev. Lett. **91**, 072 301 (2003)
27. J.L. Albacete, N. Armesto, A. Kovner, C.A. Salgado, U.A. Wiedemann, Phys. Rev. Lett. **92**, 082 001 (2004)
28. V. Topor Pop, M. Gyulassy, J. Barrette, C. Gale, S. Jeon, R. Bellwied, Phys. Rev. C **75**, 014 904 (2007)
29. E.L. Bratkovskaya et al., Phys. Rev. C **69**, 054 907 (2004)